PHYSICAL REVIEW E **74**, 040801(R) (2006)

Shear alignment of sphere-morphology block copolymer thin films with viscous fluid flow

Mingshaw W. Wu,[1] Richard A. Register,[2] and Paul M. Chaikin[1,3]
[1]*Department of Physics, Princeton University, Princeton, New Jersey 08544, USA*
[2]*Department of Chemical Engineering, Princeton University, Princeton, New Jersey 08544, USA*
[3]*Physics Department and Center for Soft Condensed Matter Research, New York University, New York, New York 10003, USA*
(Received 2 May 2006; published 9 October 2006)

The effect of shear on crystalline order is interesting fundamentally, as well as technologically, for producing long-range alignment of micron- and nanoscale structures. We study the influence of shear on a sphere-forming diblock copolymer thin film consisting of a stack of two to six hexagonal layers, using a stress-controlled rheometer to transmit the stress through a viscous fluid layer. Above a threshold stress, the hexagonal layers align macroscopically in the "easy shear" direction. A simple phenomenological model with an orientation-dependent order-disorder temperature, $T^*_{\mathrm{ODT}}(\delta\theta)=T_{\mathrm{ODT}}[1-(\sigma/\sigma_c)\sin^2(3\delta\theta)]$ and recrystallization describes the influence of stress level, temperature, and shearing time remarkably well.

DOI: 10.1103/PhysRevE.74.040801 PACS number(s): 61.25.Hq, 64.60.Cn

Thin films of diblock copolymers are finding application in periodic nanolithography, and as new systems for studying ordering and phase transitions in two dimensions. Typical block copolymer thin films show a polygranular structure, with a correlation length ξ that grows slowly with the annealing time, as $\xi \sim t^{1/4}$ for cylindrical [1,2] and spherical [3] morphologies. Techniques to induce long-range order and alignment include electric fields [4], and prepatterning of the surface chemistry [5] or topography [6,7]. Shear flow can align block copolymers in bulk [8–14]. In other periodic systems shear can either enhance alignment and order, or destroy it, e.g., shear melting and crystallization in granular material [15] and in colloidal crystals [16–18].

Recently, Angelescu *et al.* have macroscopically shear-aligned single-layer cylinder [19] and bilayer spherical [20] block copolymer thin films. The shear stress was transmitted with a polydimethylsiloxane (PDMS) rubber pad. Here, we present a quantitative study of the same sphere-morphology poly(styrene)-poly(ethylene-*alt*-propylene) diblock copolymer, PS-PEP 3-24. We use a rheometer (Rheometrics DSR-200) to apply the shear stress through a relatively thick film ($h=0.1-0.4$ mm) of a viscous fluid (PDMS (silicone) oil, $\eta=10^6$ centistokes, a nonsolvent for the polymer) (Fig. 1). A film containing two to six layers of spheres (order 100 nm thick) is produced by spin-coating from dilute solution onto a silicon wafer [20]. The nearly Newtonian fluid transmits a shear stress, $\sigma_{\phi z}(r)=\eta\partial v_\phi/\partial z=\eta r\omega/h$ (where v_ϕ is the tangential velocity, and ω is the rotation rate) which varies linearly with the distance r from the rotation axis. After shearing at a prescribed temperature (above T_{glass} for both blocks) for a given time, we quench the system to room temperature, remove the specimen from the rheometer and the PDMS oil from the film, and image the film near-surface structure by tapping-mode atomic force microscopy (AFM, Digital Instruments Dimension 3000).

Figure 2(a) represents the grain structure revealed by AFM on a low-stress (280 Pa) region near the center of rotation. Short black line segments in the figure represent dislocations within the hexagonal lattice; strings of these dislocations constitute the grain boundaries [3]. The parallel gray lines reflect the orientation of the hexagonal lattice within each grain with the association $\theta_{\mathrm{lines}} \leftrightarrow 3\theta_{\mathrm{hexagonal}}$. Figure 2(a) is typical of unsheared films, with ~ 1 μm grains of random orientation. Figure 2(b) represents the structure of a high-stress (3460 Pa) region. There are few dislocations and the entire image shows a strongly preferred orientation of the hexagonal lattice, with the closest-packing lines of spheres aligned with the shear velocity direction, ϕ [20]. This orientation corresponds to the "easy shear" direction illustrated in Fig. 2(c). The alignment of the spheres can be quantified through a hexagonal orientational order parameter relative to the local velocity direction, $S=\langle\cos(6\delta\theta)\rangle$, where $\delta\theta$ is the angular difference between the velocity direction, ϕ, and the "bond" connecting the centers of two neighboring spheres; $S=1$ for perfect alignment with the velocity direction, $S=-1$ for alignment at 30°, and $S=0$ for random orientation. The main panel of Fig. 2 shows the alignment parameter as a function of applied shear stress for three samples run at different rheometer rotation rates. Quantitatively similar results were obtained for films containing two or six layers of spheres as well.

Each data point in Fig. 2 is from an AFM image of 2.5 μm $\times$ 2.5 μm, a size limited by the need to resolve each sphere. At low stress each image has a few random grains of ~ 1 μm explaining the large scatter in $\delta S \sim \pm(\text{number grains})^{-1/2} \sim \pm 0.3$. When the polygrain structure is eliminated at higher stresses, the scatter in S is greatly reduced, though S does not reach unity. Small deviations in the positions of the spheres will reduce S in a Debye-Waller-like fashion. If $\delta\theta$ is evaluated by averaging over a three-unit-cell neighborhood surrounding each bond, $S \approx 0.95$ at high stress. The distortions do not disturb the long-range orientational order of the sheared lattice.

Figure 3 shows S as a function of stress for different combinations of temperature and shearing time. The data in Fig. 3 suggest a threshold stress below which the sample shows no alignment. We fit each 30 min data set to a two-parameter step function: $S=0$ for $\sigma<\sigma_{\mathrm{step}}$, $S=$constant for $\sigma>\sigma_{\mathrm{step}}$. Figure 4 shows σ_{step} versus temperature. The striking result is that the stress required for alignment goes linearly to zero at the order-disorder transition temperature T_{ODT}, 121 °C for a bulk film of PS-PEP 3-24 [21] and 125 °C for a single-layer film [22].

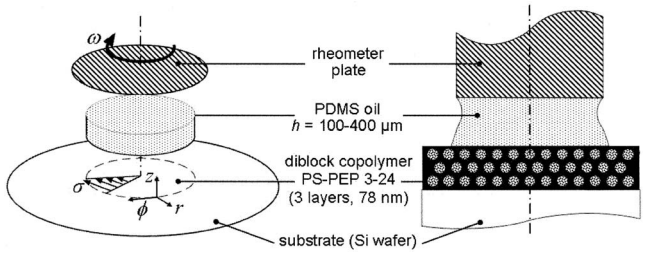

FIG. 1. Schematic of the parallel-plate rheometer setup. Left: exploded isometric view, indicating the cylindrical (shear) coordinate directions: r (vorticity), ϕ (velocity), and z (gradient). Right: cross-sectional view, not to scale: note that the PDMS oil layer is $>10^3$ times thicker than the sphere-forming block copolymer film (three hexagonal layers of spheres shown).

Though diblock copolymers in bulk are well known to align in shear, there is no general formalism for treating the problem. Often such problems are treated through simulations using a time-dependent Landau model [23,24]. The step stress for the data in Fig. 2, around 400 Pa, is comparable to the critical stress required to destroy ("melt") the lattice order in bulk PS-PEP 3-24 [25], yet here in thin films of the same polymer above the threshold stress, we get near-perfect alignment of hexagonal layers.

We propose a simple phenomenological model of orientation-dependent melting and recrystallization. The basic idea that we will use is that the effective T_{ODT} is driven down when planes are sheared over one another in a less favorable direction

$$T^*_{\mathrm{ODT}}(\delta\theta) = T_{\mathrm{ODT}}[1 - (\sigma/\sigma_c)\sin^2(3\delta\theta)]. \tag{1}$$

σ is the applied shear stress, σ_c is a characteristic stress, and $\delta\theta$ is the angle between the hexagonal lattice vector and the shear velocity direction. If a film is sheared at a temperature, T, such that $T^*_{\mathrm{ODT}}(30°) < T < T_{\mathrm{ODT}}$, then all regions of the sample with larger misalignment than $(1/3)\sin^{-1}[(T_{\mathrm{ODT}} - T)/(\sigma/\sigma_c)]^{1/2}$ will melt and recrystallize better aligned.

The reduction of T^*_{ODT} by shear can be argued within a Landau model. For clarity, we treat two layers of a square lattice here, to avoid the algebraic complexity of a hexagonal lattice. A Landau free energy expansion for the two-layer system can be written as

$$F = c[(\chi N)_{\mathrm{ODT}} - \chi N]\psi_1^2 + u\psi_1^4 + c[(\chi N)_{\mathrm{ODT}} - \chi N]\psi_2^2 + u\psi_2^4 + b\psi_1\psi_2. \tag{2}$$

Here $\psi_i = \delta\rho_i\{\cos[2\pi(x_i - x_{i,0})] + \cos[2\pi(y_i - y_{i,0})]\}$ is the order parameter for a square density modulation (amplitude $\delta\rho_i$, periodicity unity) characteristic of the lattice in layer $i=1,2$ and χ is the Flory interaction parameter, and N is the degree of polymerization [26,27]. The interlayer coupling $b(\mathbf{r}_{2,0} - \mathbf{r}_{1,0}, \Omega)$ depends on the relative displacements, $\mathbf{r}_{2,0} - \mathbf{r}_{1,0}$, and orientations, Ω, of the lattices in the two layers: $x_2 = x_{2,0} - x_{1,0} + x_1\cos(\Omega) + y_1\sin(\Omega)$, $y_2 = y_{2,0} - y_{1,0} - x_1\sin(\Omega) + y_1\cos(\Omega)$. Steric effects between the spherical microdomains lead to repulsive interactions so that a sphere in one layer prefers to sit in the center of the square defined by the spheres in the other layer. This will lead to a minimum in coupling energy when $\Omega=0$, $x_{2,0} - x_{1,0} = y_{2,0} - y_{1,0} = \frac{1}{2}$. If we take the repulsion as a delta function, $\delta(\mathbf{r}_2 - \mathbf{r}_1)$, and $\Omega=0$, then $b = (\frac{1}{2})\{\cos[2\pi(x_{2,0} - x_{1,0})] + \cos[2\pi(y_{2,0} - y_{1,0})]\}$. For any finite Ω, $b=0$, as x and y periodicities are incommensurate.

Typically, χ is a decreasing function of temperature, often expressed as $\chi = A/T + B$ with $A > 0$, so that the material is ordered below T_{ODT} and disordered above T_{ODT}. Since N is a constant for a given polymer, we may thus rewrite Eq. (2) for temperatures near T_{ODT} as

$$F = a(T - T_{\mathrm{ODT}})\psi_1^2 + u\psi_1^4 + a(T - T_{\mathrm{ODT}})\psi_2^2 + u\psi_2^4 + b\psi_1\psi_2, \tag{3}$$

where a has the same sign as A, the temperature coefficient of χ. Further, since the two layers are equivalent, we expect a transition with $\psi_1 = \psi_2 = \psi$, so Eq. (3) becomes

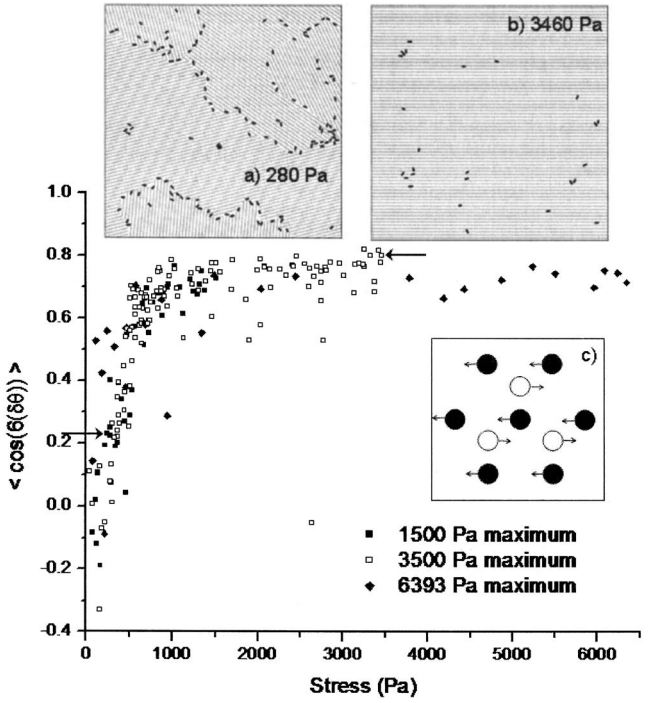

FIG. 2. Main panel: alignment parameter $S = \langle\cos(6\delta\theta)\rangle$, as a function of shear stress. Each datapoint represents the value of S averaged over a single 2.5 μm × 2.5 μm AFM image taken at a particular distance r from the rotation axis, corresponding to a particular value of the shear stress. Data from three different shearing experiments are shown, as indicated in the legend, where the shear stresses at the rim of the rheometer plate are given. (a) Grain structure revealed by an AFM image (2.5 μm × 2.5 μm) of a region at low applied shear stress (280 Pa). Short black line segments represent dislocations, which collectively define the grain boundaries. Gray shading lines represent the orientation of the hexagonal lattice; a 180° rotation of the shading lines corresponds to a 60° rotation of the hexagonal lattice. (b) Analogous representation of a region at high applied shear stress (3460 Pa). Note absence of grain boundaries. (c) Schematic of the "easy shear" direction, where spheres in the upper layer (open circles) move in the interstices of the hexagonal lower layer.

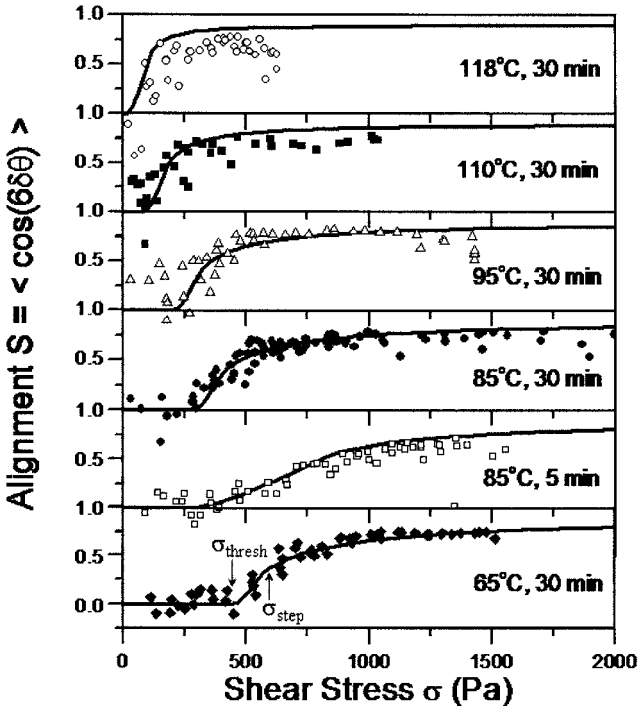

FIG. 3. Alignment parameter S as a function of applied shear stress for different temperatures and shear durations, as indicated in each panel; vertical range of each panel is $0 \leqslant S \leqslant 1$. Points are experimental data and solid curves are fits to our phenomenological model. Threshold and step stresses, σ_{thresh} and σ_{step}, are indicated by vertical arrows in the bottom panel.

$$F = a'(T - T_{\text{ODT}})\psi^2 + u'\psi^4 + b\psi^2 = a'(T - T^*_{\text{ODT}})\psi^2 + u'\psi^4, \tag{4}$$

where $a' = 2a$, $u' = 2u$, and $T^*_{\text{ODT}} = T_{\text{ODT}} - b/a'$. Equation (4) shows that the interlayer coupling enters as an apparent shift of T_{ODT}, by an amount dependent on b. The treatment thus far is for equilibrium. As an approximation to the effects of shear, we displace the layers relative to one another linearly in time, t, by $x_{2,0} - x_{1,0} = \dot{\gamma} t \cos(\delta\theta)$, $y_{2,0} - y_{1,0} = \dot{\gamma} t \sin(\delta\theta)$ and time-average assuming an order parameter relaxation time of τ_R. From symmetry and the relaxation time approximation we expect b to be a function of $4\delta\theta$ and $\dot{\gamma}\tau_R$. For our rigid bilayer model b is finite only for $\delta\theta = 2\pi n/4$ with integer n, but for a more realistic model we expect b to vary smoothly with $\delta\theta$. We assume the simple functional form $b \sim \dot{\gamma}\tau_R \sin^2(2\delta\theta)$. Since we expect τ_R to be proportional to viscosity, $\dot{\gamma}\tau_R$ is proportional to the shear stress σ, so that the product $a' T_{\text{ODT}}$ then defines a characteristic stress σ_c. Substituting these expressions into that for T^*_{ODT} and changing to hexagonal symmetry ($2\delta\theta \to 3\delta\theta$) leads to Eq. (1).

To complete the model, we add the simplest time dependence of the melting and subsequent recrystallization processes [28]. An area $R(\delta\theta)$ above its local melting temperature ($T > T^*_{\text{ODT}}$) melts at a rate $\partial R(\delta\theta)/\partial t = \Gamma[T^*_{\text{ODT}}(\delta\theta) - T]/T_{\text{ODT}}$, and the material in that melted area recrystallizes with an orientation distribution governed by the same rate law, $\partial R(\delta\theta)/\partial t = \Gamma[T^*_{\text{ODT}}(\delta\theta) - T]/T_{\text{ODT}}$, into orientations $\delta\theta$

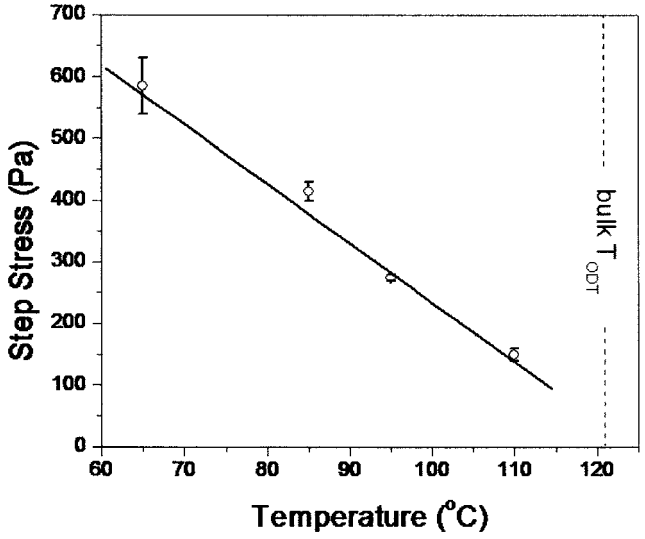

FIG. 4. Step stress, determined by fitting the 30 min data in Fig. 3 to a step function, against shearing temperature. The bulk order-disorder transition temperature ($T_{\text{ODT}} = 121\ ^\circ\text{C}$) is indicated by the vertical dashed line. Uncertainty intervals reflect the discreteness of the stress values in Fig. 3: the best-fit step stress falls between the values for two adjacent data points, represented as the ends of the error bars.

where $T^*_{\text{ODT}}(\delta\theta) > T$ [28]. After an elapsed time t the areal distribution is given by

$$R(\delta\theta) = R(\delta\theta)_{\text{initial}}[1 + t\Gamma(T^*_{\text{ODT}}(\delta\theta) - T\ ]/\ T_{\text{ODT}}) \quad \text{for } T > T^*_{\text{ODT}}(\delta\theta), \quad R(\delta\theta) \geqslant 0,$$

$$R(\delta\theta) = R(\delta\theta)_{\text{initial}}\{1 + t\Gamma\beta[T^*_{\text{ODT}}(\delta\theta) - T]/T_{\text{ODT}}\} \quad \text{for } T < T^*_{\text{ODT}}(\delta\theta). \tag{5}$$

We assume the initial distribution of areas $R(\delta\theta)_{\text{initial}}$ is independent of $\delta\theta$; β is a scale factor adjusted to keep the total area conserved.

The working parts of this model are Eqs. (1) and (5). Equation (1) describes two important features of the data immediately. First, a threshold stress: only when the stress is raised to the level where $T^*_{\text{ODT}}(30^\circ) = T$ will the most misaligned regions start to melt. Second, the value of this threshold stress should decrease linearly to zero as T approaches T_{ODT}, consistent with the behavior of the step stress shown in Fig. 4.

A more detailed comparison of this phenomenological model with experimental data requires the determination of three parameters: σ_c, Γ, and a Debye-Waller-like factor D, which rescales S at saturation to experiment. To obtain these three parameters, we fit the $T = 85\ ^\circ\text{C}$ and $t = 5$ min data set, obtaining $\sigma_c = 3200$ Pa, $\Gamma = 0.02\ \text{sec}^{-1}$, and $D = 0.9$. We then held these parameters fixed and calculated the S vs σ (Fig. 3 continuous curves). The agreement of the model with the experimental data is striking, given its simplicity.

Some discussion of the parameter values is in order. We used a fixed $\Gamma = 0.02\ \text{sec}^{-1}$, but we expect $\Gamma \propto D_s(T)$ a self-diffusion coefficient. Fits using reasonable estimates of $\Gamma(T)$

are not significantly different from those presented because the higher temperature data is already in the long-time, saturated limit, $\Gamma t > 10$. The characteristic stress σ_c is within an order of magnitude of the critical stress required to destroy the lattice when shearing bulk specimens. The bulk critical stress is only weakly dependent on temperature, and does not go to zero at T_{ODT} [25]. Previous models for shear alignment often deal with lamellar systems where ODT increases due to a shear induced reduction in fluctuations, a mechanism inappropriate for crystalline systems and especially bilayers [29].

To summarize, we have performed the first shear alignment of diblock copolymer films using a viscous fluid to transmit the stress, an approach that allowed us to measure the alignment as a continuous function of stress on a single sample. Our experimental results show a temperature—dependent threshold stress above which films containing two to six layers of hexagonally-packed spherical microdomains begin to align. The threshold stress goes to zero at T_{ODT}. We have also presented a phenomenological model with an orientation- and stress-dependent effective order-disorder temperature: the essence of the model is that misaligned regions shrink at the expense of aligned regions, there is a threshold stress for alignment to occur, and that the threshold stress goes to zero at T_{ODT}. We emphasize that many models will give the first two dependences but the last is rather constraining. Diblock copolymer films may be excellent systems for understanding some aspects of nonequilibrium driven systems.

We thank Robert Prud'homme and Xuhong Guo for assistance with the rheometer experiments, and David Huse and Scott Milner for helpful discussions. Support for this work was provided by the NSF MRSEC Program through the Princeton Center for Complex Materials (DMR-0213706).

[1] C. Harrison, D. H. Adamson, Z. Cheng, J. M. Sebastian, S. Sethuraman, D. A. Huse, R. A. Register, and P. M. Chaikin, Science **290**, 1558 (2000).

[2] C. Harrison, Z. Cheng, S. Sethuraman, D. A. Huse, P. M. Chaikin, D. A. Vega, J. M. Sebastian, R. A. Register, and D. H. Adamson, Phys. Rev. E **66**, 011706 (2002).

[3] C. Harrison, D. E. Angelescu, M. Trawick, Z. Cheng, D. A. Huse, P. M. Chaikin, D. A. Vega, J. M. Sebastian, R. A. Register, and D. H. Adamson, Europhys. Lett. **67**, 800 (2004).

[4] T. L. Morkved, M. Lu, A. M. Urbas, E. E. Ehrichs, H. M. Jaeger, P. Mansky, and T. P. Russell, Science **273**, 931 (1996).

[5] S. O. Kim, H. H. Solak, M. P. Stoykovich, N. J. Ferrier, J. J. de Pablo, and P. F. Nealey, Nature (London) **424**, 411 (2003).

[6] R. A. Segalman, H. Yokoyama, and E. J. Kramer, Adv. Mater. (Weinheim, Ger.) **13**, 1152 (2002).

[7] J. Y. Cheng, C. A. Ross, E. L. Thomas, H. I. Smith, and G. J. Vancso, Appl. Phys. Lett. **81**, 3657 (2002).

[8] G. Hadziioannou, C. Picot, A. Skoulios, M.-L. Ionescu, A. Mathis, R. Duplessix, Y. Gallot, and J.-P. Lingelser, Macromolecules **15**, 263 (1982).

[9] Z.-R. Chen, J. A. Kornfield, S. D. Smith, J. T. Grothaus, and M. M. Satkowski, Science **277**, 1248 (1997).

[10] A. Keller, E. Pedemonte, and F. M. Willmouth, Nature (London) **225**, 538 (1970).

[11] D. B. Scott, A. J. Waddon, Y.-G. Lin, F. E. Karasz, and H. H. Winter, Macromolecules **25**, 4175 (1992).

[12] M. E. Vigild, K. Almdal, K. Mortensen, I. W. Hamley, J. P. A. Fairclough, and A. J. Ryan, Macromolecules **31**, 5702 (1998).

[13] K. Almdal, K. A. Koppi, and F. S. Bates, Macromolecules **26**, 4058 (1993).

[14] E. Eiser, F. Molino, G. Porte, and O. Diat, Phys. Rev. E **61**, 6759 (2000).

[15] J.-C. Tsai, G. A. Voth, and J. P. Gollub, Phys. Rev. Lett. **91**, 064301 (2003).

[16] R. L. Hoffman, J. Colloid Interface Sci. **46**, 491 (1974).

[17] B. J. Ackerson, J. B. Hayter, N. A. Clark, and L. Cotter, J. Chem. Phys. **84**, 2344 (1986).

[18] B. J. Ackerson and P. N. Pusey, Phys. Rev. Lett. **61**, 1033 (1998).

[19] D. E. Angelescu, J. H. Waller, D. H. Adamson, P. Deshpande, S. Y. Chou, R. A. Register, and P. M. Chaikin, Adv. Mater. (Weinheim, Ger.) **16**, 1736 (2004).

[20] D. E. Angelescu, J. H. Waller, R. A. Register, and P. M. Chaikin, Adv. Mater. (Weinheim, Ger.) **17**, 1878 (2005).

[21] D. E. Angelescu, C. K. Harrison, M. L. Trawick, P. M. Chaikin, R. A. Register, and D. H. Adamson, Appl. Phys. A **78**, 387 (2004).

[22] D. E. Angelescu, C. K. Harrison, M. L. Trawick, R. A. Register, and P. M. Chaikin, Phys. Rev. Lett. **95**, 025702 (2005).

[23] Y. Oono and S. Puri, Phys. Rev. Lett. **58**, 836 (1987).

[24] D. A. Vega, C. K. Harrison, D. E. Angelescu, M. L. Trawick, D. A. Huse, P. M. Chaikin, and R. A. Register, Phys. Rev. E **71**, 061803 (2005).

[25] J. M. Sebastian, C. Lai, W. W. Graessley, and R. A. Register, Macromolecules **35**, 2707 (2002).

[26] L. Leibler, Macromolecules **13**, 1602 (1980).

[27] M. W. Matsen and F. S. Bates, Macromolecules **29**, 7641 (1996).

[28] If we take $R(\delta\theta)/\partial t = R(\delta\theta)\Gamma[T^{*}_{\mathrm{ODT}}(\delta\theta) - T]/T_{\mathrm{ODT}}$ there is a slight quantitative change in the data fits even retaining the same parameters.

[29] M. E. Cates, and S. T. Milner, Phys. Rev. Lett. **62**, 1856 (1989).